


## Article

# Mitigation of Urban Heat Island Effects by Thermo-chromic Asphalt Pavement

Orlando Lima, Jr. <sup>1</sup>, Elisabete Freitas <sup>1,\*</sup>, Pedro Cardoso <sup>2</sup>, Iran Rocha Segundo <sup>1,3,\*</sup>, Élide Margalho <sup>1</sup>, Luís Moreira <sup>2</sup>, José Heriberto O. Nascimento <sup>4</sup>, Salmon Landi, Jr. <sup>5</sup> and Joaquim Carneiro <sup>3,\*</sup>

<sup>1</sup> Department of Civil Engineering, Institute for Sustainability and Innovation in Structural Engineering (ISISE), University of Minho, 4800-058 Guimarães, Portugal

<sup>2</sup> Department of Civil Engineering, University of Minho, 4800-058 Guimarães, Portugal

<sup>3</sup> Centre of Physics of Minho and Porto Universities (CF-UM-UP), Azurém Campus, University of Minho, 4800-058 Guimarães, Portugal

<sup>4</sup> Textile Engineering Department, Federal University of Rio Grande do Norte, Natal 59078-970, Brazil

<sup>5</sup> Federal Institute Goiano, Rio Verde 75901-970, Brazil

\* Correspondence: efreitas@civil.uminho.pt (E.F.); iran@civil.uminho.pt (I.R.S.); carneiro@fisica.uminho.pt (J.C.)

**Abstract:** Asphalt road pavements are usually dark and, consequently, have a low albedo. Therefore, they absorb energy as heat, increasing the Urban Heat Island (UHI) effect, which impacts the environment, energy consumption, and human health. Through the functionalization with thermo-chromic materials (TM), this work aims to develop a smart asphalt pavement able to change its surface color, increasing the reflectance, and thus mitigate this phenomenon. To achieve this goal, asphalt substrates were functionalized by a surface spray coating of a thermo-chromic solution (TS) containing aqueous solution of thermo-chromic microcapsules (thermocapsules), dye, and epoxy resin. To evaluate the functionalization features, Fourier Transform Infrared Spectroscopy (FTIR), and Thermal Differential test (TDT) with cyclic temperature variation were performed in the functionalized asphalt binder. Moreover, Scanning Electron Microscopy (SEM), Energy-Dispersive X-ray Spectrometry (EDS), a Quick Ultraviolet Accelerated Weathering Test (QUV) with Colorimetry test, and an adaptation of the Accelerated Polishing Test (APT) were performed on the functionalized asphalt mixture. The results indicate that the functionalization of asphalt substrates with TS exhibits a reversible color-change ability, higher luminosity values when subjected to temperatures above 30 °C, and wear resistance.

**Keywords:** thermo-chromism; smart asphalt pavement; cool pavements; thermocapsules; Leuco dyes



**Citation:** Lima, O., Jr.; Freitas, E.; Cardoso, P.; Segundo, I.R.; Margalho, É.; Moreira, L.; O. Nascimento, J.H.; Landi, S., Jr.; Carneiro, J. Mitigation of Urban Heat Island Effects by Thermo-chromic Asphalt Pavement. *Coatings* **2023**, *13*, 35. <https://doi.org/10.3390/coatings13010035>

Academic Editor: Valeria Vignali

Received: 9 November 2022

Revised: 8 December 2022

Accepted: 22 December 2022

Published: 25 December 2022



**Copyright:** © 2022 by the authors. Licensee MDPI, Basel, Switzerland. This article is an open access article distributed under the terms and conditions of the Creative Commons Attribution (CC BY) license (<https://creativecommons.org/licenses/by/4.0/>).

## 1. Introduction

Urban Heat Islands (UHI) are defined by the occurrence of higher temperatures in urban areas compared to the surrounding rural environment and have been considered one of the most significant problems in the current century. This phenomenon has as main causes human activities, such as: replacement of vegetation by infrastructure (buildings and road pavements) with high solar absorption, soil impermeability, energy storage, and heat release, presenting a high impact on the environment, energy needs, and human health [1–3]. The dark coloration of road pavements, which presents a low albedo, is a strong contributing factor to increased temperatures in urban centers [4]. Albedo is the fraction of solar energy received by the Earth that is returned scattered to space and ranges from 0 (100% absorption and 0% reflection) to 1 (0% absorption and 100% reflection). The albedo of a surface is the fraction of incident sunlight that this surface reflects; the fraction not reflected is absorbed, which causes the increase in surface temperature [5,6]. Some mitigation measures have been studied to avoid the UHI effect, such as: increasing the use of green spaces within the urban area, exploring the cooling effects of wind and water, and designing cool pavements with more reflective (increased albedo), permeable porous, and water-retaining properties [7,8]. The solar reflective coating is one common

alternative concerning cool pavements due to its ease of implementation and its cost-benefit advantages [9].

Thermochromic (TM) materials show color changes in their visible optical properties upon temperature changes and, due to this, can be used in solar reflective pavement coatings. The color change process occurs at a specific transition temperature (TT) as a result of a chromogenic core. TM can be classified into two groups concerning the mechanisms of thermochromic behavior: (i) dye-based, and (ii) non-dye. The first group works through proton transfer of dyes embedded in a polymer matrix or through proton transfer reactions in Leuco dyes. The second group presents a color change associated with nanometric scale and molecular rearrangements by temperature change [10–15]. The Leuco dye systems can go from the colored state to the colorless and consist of three components: color former (Leuco dye), color developer, and co-solvent. The melting point of the co-solvent determines the TT; the material is colored below its melting point and becomes colorless above this temperature (Figure 1). These systems have a low production cost and a TT compatible with the temperature range of the construction sector. For this reason, they have been widely used in this industry [16] as well as in the aerospace, military, textile, and other industries [17]. Their main disadvantage is the fast aging [18] due to ultraviolet radiation exposure, which decreases the thermochromic capacity [19]. For this reason, microencapsulation is a strategy to hold the entire thermochromic system together, protecting it from the surrounding environment, reducing its volatility, and improving its stability [20,21].

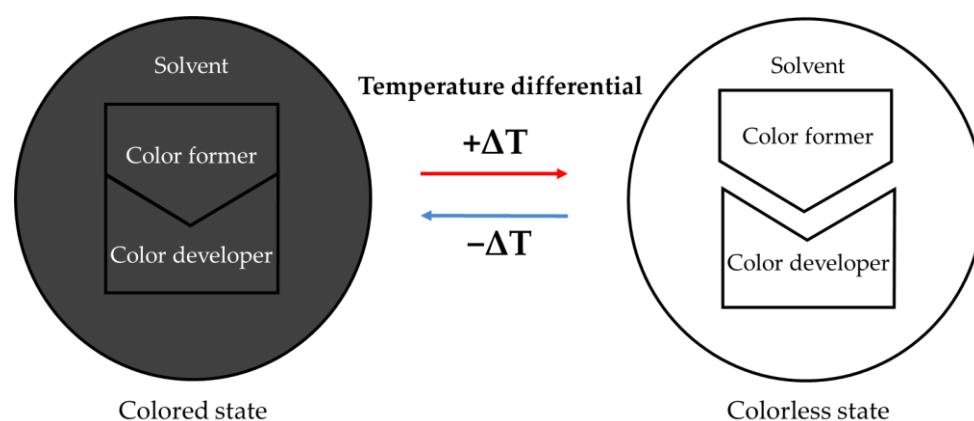


**Figure 1.** The thermochromic mechanism in Leuco dyes [11].

In general, reflective pavements can be developed by applying a coating with highly reflective, infra-red reflective, or thermochromic properties, as well as by using heat reflective coated aggregates, or fly ash and slag in the case of concrete cement pavement [22]. For example, titanium dioxide ( $\text{TiO}_2$ ) and epoxy resin were used in the asphalt pavement as a solar reflective coating and reduced the surface temperature from 71.3 to 57.9 °C [23]. In another study, silica,  $\text{TiO}_2$ , diatomite, hollow glass beads, and epoxy resin were used as the solar reflective coating, and a reduction of about 11 °C of the surface temperature was achieved [24]. Reversible thermochromic microcapsules were used in the development of reflective pavements and achieved a cooling effect that could reach 10.57 °C [25]. Asphalt binders were also functionalized by mixing thermochromic microcapsules, and optical and mechanical properties were improved; recommended concentrations were around 5%–6% [26]. However, most studies concern the temperature variation control and are mainly focused on the durability of the asphalt pavements and the mechanical characteristics of asphalt mixtures once high temperatures contribute to the permanent deformation process of the asphalt pavements, and the low temperatures are associated with cracking and ice formation [1,27–30].

Therefore, in the asphalt paving field, the functionalization with TM is still scarce, but controlled color variation and increased reflectivity of thermochromic pavements can

mitigate the UHI effects [1]. However, this modification can be achieved by functionalizing the asphalt mixtures with a thermochromic capability. Figure 2 compares a conventional asphalt pavement (low albedo) and a thermochromic pavement (high albedo). In conventional asphalt, due to its dark color, a large amount of the incident solar radiation is absorbed by the pavement, contributing to the heating of urban centers [1]. In contrast, by incorporating a thermochromic layer, a higher solar reflectivity at high temperatures is achieved, which lowers the surface temperature and reduces energy absorption in the form of heat by the pavement [25].

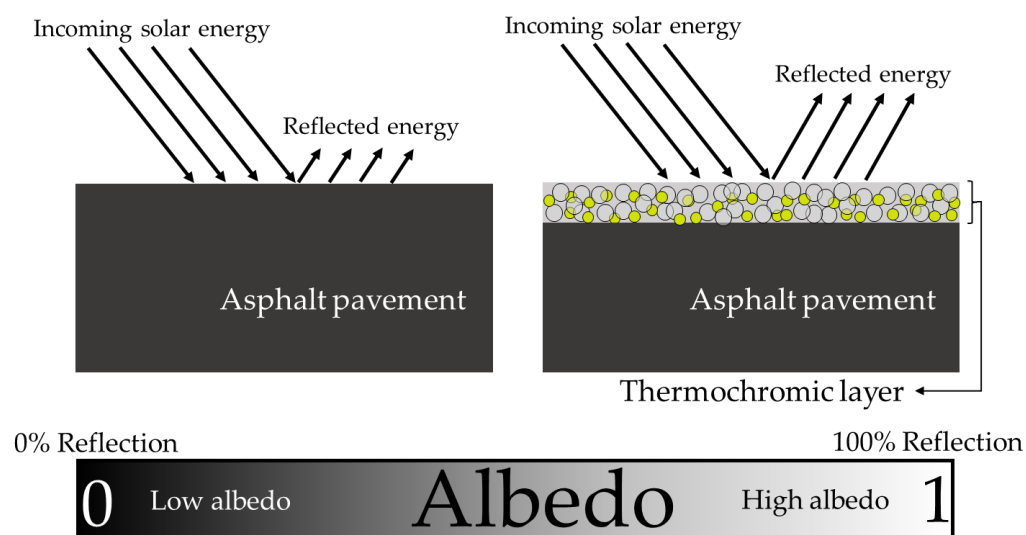


**Figure 2.** Asphalt pavement with thermochromic ability.

Considering that the reflectivity of asphalt mixtures can be increased with the introduction of TM due to the color change based on temperature variation [27], this work aims to develop a solution capable of reducing the absorption of energy in the form of heat by asphalt pavements, and, consequently, reduce the UHI effects. To this end, it is proceeded by the functionalization of asphalt substrates (asphalt binder and asphalt mixture) by spraying a thermochromic solution (TS) containing thermochromic particles (thermocapsules), dye, and epoxy resin, whose temperature sensitivity leads to color change.

## 2. Materials and Methods

### 2.1. Materials

The materials used in this research were: (i) commercial thermocapsules (ChromaZone<sup>®</sup>—color-changing, heat-sensitive) (Flintshire, Great Britain), (ii) yellow dye, (iii) epoxy resin, (iv) asphalt binder Elaster 13/60, and (v) asphalt mixture AC 10.

### 2.2. Sample Preparation

The asphalt binder and the asphalt mixture were functionalized by spraying the surface with TS containing thermocapsules and dye at concentrations recommended by the suppliers and previously indicated in the literature to have better optical, mechanical, and surface performance [24,26,31–36]. In order to improve the immobilization of the thermocapsules over the asphalt pavements, a resin was also used to compose the solutions for spraying. Thus, two approaches were carried out; one without resin and another with. The first is composed of an aqueous solution of thermocapsules (3% *w/v*) and yellow dye (0.5% *w/v*). The second one consists of thermocapsules (3% *w/v*), yellow dye (0.5% *w/v*), and epoxy resin (20 mL). The insertion of the yellow dye in the TS is justified by the color of the pavement. When the temperatures are above 30 °C, the thermocapsules, initially with a dark coloration (similar to the pavement), become colorless, showing the yellow dye. After the discoloration of these thermocapsules, the color of the dye will be perceived over

the asphalt substrate. If the dye had not been inserted into the TS, only the dark color in the substrate would be perceived. The behavior of the TS on the asphalt substrate is shown in Figure 3.

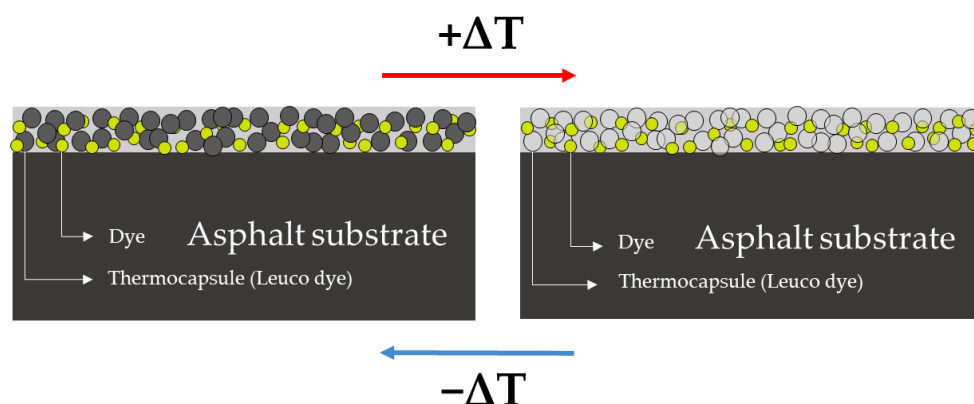


**Figure 3.** Asphalt substrate functionalized with the thermochromic solution.

### 2.3. Test Methods, Experimental Equipment, and Conditions

The tests occurred in two stages. First, the functionalization with TS was performed over the asphalt binder and then over the asphalt mixture. Thus, the characterization of the functionalized asphalt substrates was performed by observing the functioning of the TS, the consequences of its application on the substrates, and its conditions of immobilization.

For the characterization of the functionalized asphalt binder, the Fourier Transform Infrared Spectroscopy (FTIR, Shimadzu, Kyoto, Japan) in a spectral range from 400 to 4000  $\text{cm}^{-1}$  was performed to obtain the information about the chemical bonds resulting from the functionalization [32]. The Thermal Differential test was carried out to analyze macroscopically the thermal activation and reversibility of the TS above the asphalt substrate. The samples were subjected to temperatures from approximately 20–25 °C (ambient) to −10 °C, then to +40 °C and again to −10 °C.

The asphalt binder specimens functionalized with solutions containing the combination of thermocapsules, dye, and resin, were labeled as follows:

- AB: Asphalt binder.
- AB+T: Asphalt binder sprayed with an aqueous solution of thermocapsules.
- AB+D: Asphalt binder sprayed with an aqueous solution of dye.
- AB+R: Asphalt binder sprayed with a solution containing resin.
- AB+T+D: Asphalt binder sprayed with an aqueous solution of thermocapsules and dye.
- AB+T+D+R: Asphalt binder sprayed with an aqueous solution of thermocapsules, dye and resin.

For the characterization of the functionalized asphalt mixture, the analysis of the surface morphological characteristics through Scanning Electron Microscopy (SEM, FEI, Hillsboro, OR, USA) and the semi-quantitative analysis of the chemical composition through Energy-Dispersive X-ray Spectrometer (EDS, EDAX, Mahwah, NJ, USA) were performed. The simulation of environmental degradation was tested via the Quick Ultraviolet Accelerated Weathering Test (QUV) through the incidence of fluorescent lamps and UV lamps, at a temperature of 30 °C and for a period of 48 h. The Colorimetry test analysis was performed by measuring color coordinates for residence times in the QUV test equal to 0 and 48 h to numerically measure the color changes of the specimens when subjected to the QUV test conditions. The color coordinates were measured using the Minolta CM-2600d portable Spectrophotometer equipment, providing a perception of the color values of the samples at the end of this time interval, in terms of  $L^*$ ,  $a^*$ , and  $b^*$ , as defined by the Comissione Internationale de l'Éclairage (CIE), as well as  $\Delta E^*$ , which

works as a perceptibility factor and indicates the value of the color difference, but not the direction [14,37,38] (Equation (1)).

$$\Delta E^* = \sqrt{(\Delta L^*)^2 + (\Delta a^*)^2 + (\Delta b^*)^2} \quad (1)$$

$L^*$  represents the variation from black ( $L^* = 0$ ) to white ( $L^* = 100$ ),  $a^*$  the variation from red (+) to green (−), and  $b^*$  the variation from yellow (+) to blue (−). The variation of each coordinate will be calculated by comparing the initial and final coordinates of the functionalized asphalt mixture surfaces.

Finally, the wear resistance was studied through the Accelerated Polishing test (ASTM D3319-97) [39]. This test was adopted to simulate aggressive road traffic conditions. The functionalized asphalt mixtures with TS containing thermocapsules, dye, and resin were subjected to a period of immersion in water of three days at 40 °C. Subsequently, the samples were subjected to three cycles of a duration of one hour each at 300 rpm, and the TS immobilization conditions on the asphalt mixture surface were evaluated.

The asphalt mixture specimens functionalized with solutions containing the combination of thermocapsules, dye, and resin were labeled as follows:

- AM: Asphalt mixture.
- AM+T: Asphalt mixture sprayed with an aqueous solution of thermocapsules.
- AM+D: Asphalt mixture sprayed with an aqueous solution of dye.
- AM+T+R: Asphalt mixture sprayed with an aqueous solution of thermocapsules and resin.
- AM+D+R: Asphalt mixture sprayed with an aqueous solution of dye and resin.
- AM+T+D: Asphalt mixture sprayed with an aqueous solution of thermocapsules and dye.
- AM+T+D+R: Asphalt mixture sprayed with an aqueous solution of thermocapsules, dye, and resin.

Figure 4 schematizes the steps of this investigation concerning the tests performed on each functionalized asphalt substrate to achieve the desired goals.

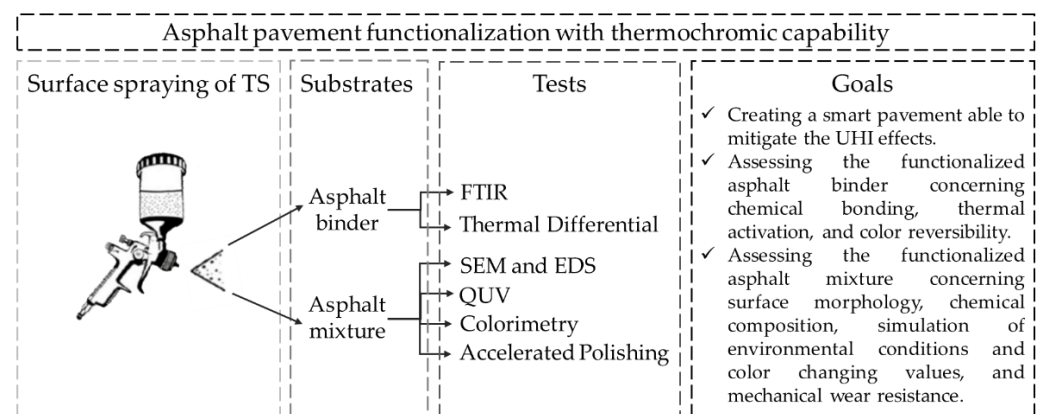


Figure 4. Schematic representation of the research.

### 3. Results and Discussion

#### 3.1. Fourier Transform Infrared Spectroscopy on Asphalt Binder

Figure 5 shows the Fourier Transform Infrared Spectroscopy (FTIR) spectra of the asphalt binder samples AB+T+D+R, AB+D, AB+T, AB, and AB+R. The spectra allow several transmittance peaks to be distinguished and associated with the vibration modes of the molecular bonds, and the main aspects of the functionalization are observed. Transmittance concerns the fraction of incident light which passes through the sample and is transmitted [40].



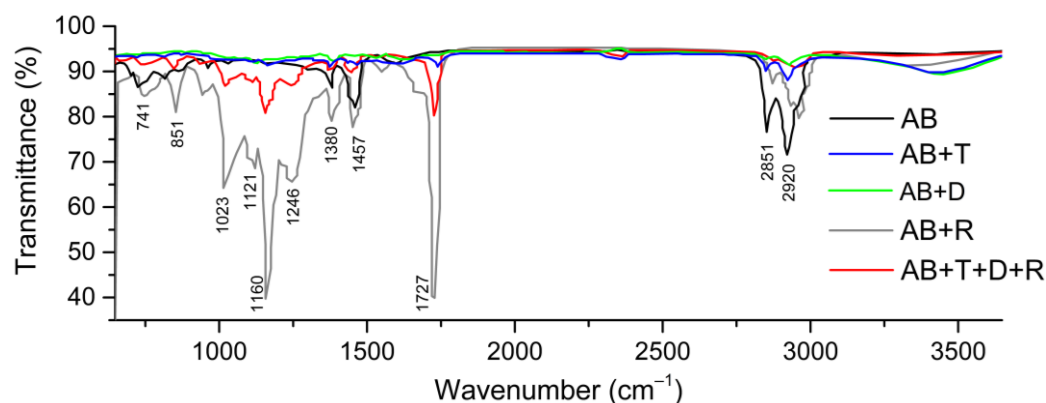


**Figure 5.** FTIR spectra of the asphalt binder sample AB and the functionalized asphalt binder samples AB+T+D+R, AB+D, AB+T, and AB+R.

Among the prominent peaks identified, it can be noticed that the FTIR spectra of the samples present strong bands attributed to the asphalt binder and the epoxy groups. The bands at 1300–1500 and 2675–3115  $\text{cm}^{-1}$ , in which are identified the peaks at 1457, 2920 and 2851  $\text{cm}^{-1}$ , respectively, are characteristic of the stretching and bending modes of saturated aliphatic hydrocarbons [41,42]. These peaks exist in most samples analyzed; however, in samples AB and AB+R, the peaks have a higher intensity, indicating the absence or lesser influence of the thickness of the functionalization layer on the representative bonds of the asphalt binder elements. The samples AB+R and AB+T+D+R, which contain resin in the functionalization solution, show peaks at 1246  $\text{cm}^{-1}$  due to ether bonds [43], strong bands at 1121 and 1160  $\text{cm}^{-1}$  corresponding to the stretching CO-C asymmetric and symmetric vibrations, and at 1727  $\text{cm}^{-1}$  regarding C=O stretching of esters, which can be useful for epoxy group identification [44,45]. The peaks at 741 and 1380  $\text{cm}^{-1}$  correspond to the characteristic vibrations of  $\text{CH}_2$  and  $\text{CH}_3$ , respectively [46,47]. Finally, the peaks at 1023 and 851  $\text{cm}^{-1}$  are also due to the resin insertions on the surface functionalization and correspond, respectively, to phenolic C-O stretching of the epoxy group and C-O-C stretching of the oxirane group [45,48].

In general, the samples in which resin was added to the surface functionalization (AB+R and AB+T+C+R) have the characteristic peaks of the epoxy groups. The characteristic peaks of the chemical bonds from the elements that compose the asphalt binder appear with considerably less expressiveness when there is a layer of TS on it, mainly containing thermocapsules or dye, such as AB+T, AB+D, and AB+T+D+R. The reduction of the characteristic peaks of the asphalt binder is weaker in the AB+R sample, and the peaks from the epoxy groups are the highest of all the samples.

This technique proved the presence of solutions that contain the combination of resin, thermocapsules, and dye on the surface of the asphalt substrate. Therefore, it ensured the occurrence of the surface functionalization.

### 3.2. Thermal Differential on Asphalt Binder

In order to demonstrate the thermochromatic capacity of the surface coating under study, as well as its color reversibility, the asphalt binders functionalized with the solution combinations AB+T+D+R, AB+T+D, AB+T, and AB+D were subjected to varied temperature conditions.

First, the samples, which were at approximately 20 to 25  $^{\circ}\text{C}$ , were cooled to  $-10$   $^{\circ}\text{C}$ . Subsequently, the samples were heated to 40  $^{\circ}\text{C}$ . Then, again, the temperature was reduced to  $-10$   $^{\circ}\text{C}$ , as indicated in Figure 6. In this way, it was possible to analyze the thermal activation and color reversibility of the TS over the asphalt binder.

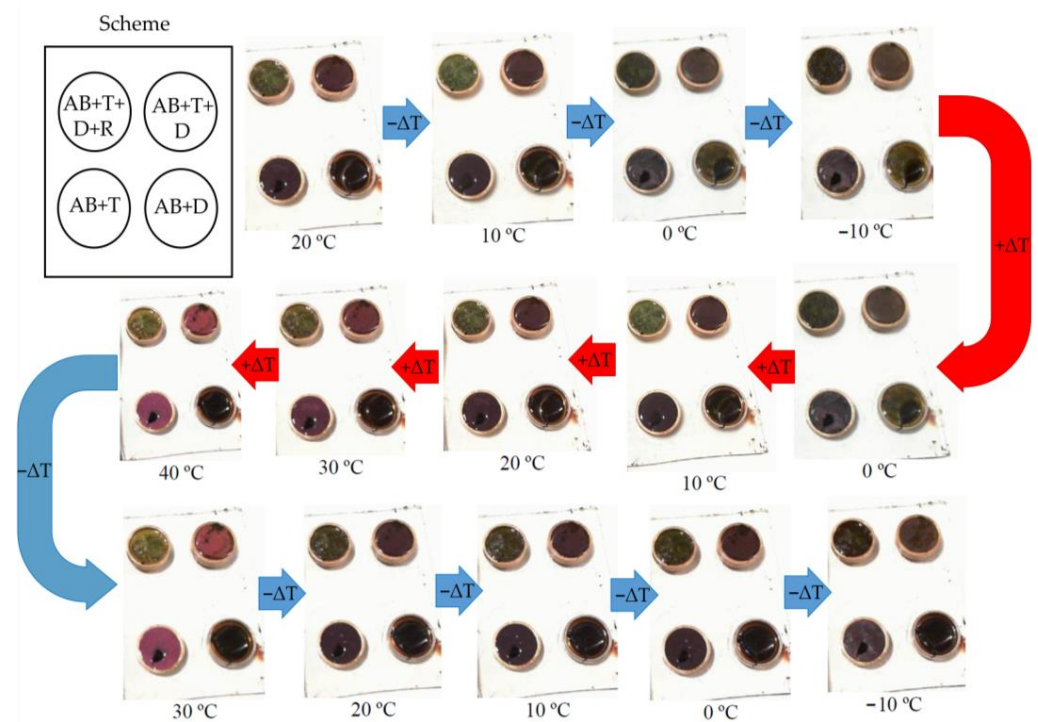


**Figure 6.** Thermal differential test of the functionalized asphalt binder samples AB+T+D+R, AB+T+D, AB+T, and AB+D.

A visual analysis of the functionalized samples submitted to thermal gradient identified a color variation during this process. Confronted with a negative temperature of  $-10\text{ }^{\circ}\text{C}$ , up to approximately  $10\text{ }^{\circ}\text{C}$ , in the solutions AB+T+D+R, AB+T+D, and AB+T, the color observed is predominantly dark, while the thermocapsules (dark-colored) are still in their colored state. From  $20$  to  $40\text{ }^{\circ}\text{C}$ , the solutions AB+T+D+R and AB+T+D show large differences in coloration, becoming lighter once the thermocapsules start their discoloration process, going from colored to colorless. At low temperatures, the thermocapsules suppress the color of the dye. At about  $30\text{ }^{\circ}\text{C}$ , the thermocapsules become colorless and, consequently, the visualization of the dye is possible. The solution AB+T is susceptible to coloration changes only at temperatures above  $30\text{ }^{\circ}\text{C}$ , consequently causing the color to disappear at lower temperatures. The sample AB+D maintained the same coloration throughout the thermal transition due to the absence of thermocapsules. After reaching  $40\text{ }^{\circ}\text{C}$ , the temperature was reduced again to  $-10\text{ }^{\circ}\text{C}$ , and the color reversibility was verified.

### 3.3. Scanning Electron Microscopy and Energy-Dispersive X-ray Spectrometer on Asphalt Mixture

The asphalt mixture samples AM, AM+T, AM+D, AM+T+D, and AM+T+D+R were subjected to Scanning Electron Microscopy (SEM) and Energy-Dispersive X-ray Spectrometer (EDS) tests. Inferences concerning changes in their surface morphology and chemical composition can be drawn from the SEM micrographs, and the EDS spectra are shown in Figure 7.

In the SEM micrograph of the specimen without functionalization, AM, the elements of the asphalt mixture surface can be seen: the asphalt binder and the aggregates. In the EDS spectrum, it is possible to identify the most significant peaks of the chemical elements present in the asphalt mixture, especially those existing in the aggregates, such as calcium (Ca) and silicon (Si).

By comparing the SEM micrographs of sample AM with AM+T and AM+D, it is possible to visually notice that there is a change in their surface and the substrate became less visible due to the functionalization layer. The EDS spectra corroborate this inference, since the peaks of the elements constituting the asphalt mixture aggregates, Si and Ca,

are less intensive, mainly in specimen AM+T. It can also be noted that the specimen that receives the thermocapsules in the functionalization layer has a significant increase in the carbon (C) amounts attributed to the TM presence.

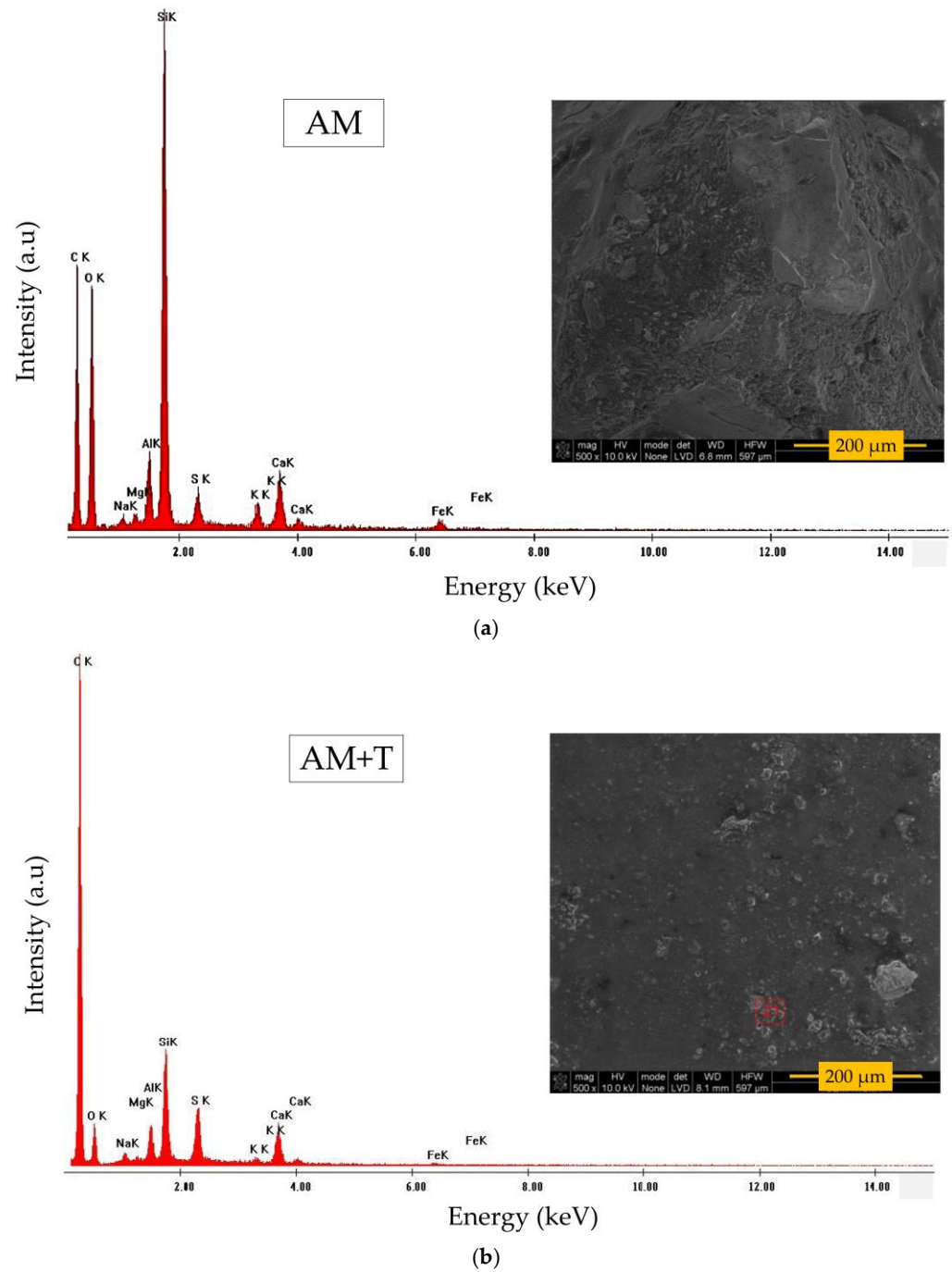


Figure 7. Cont.



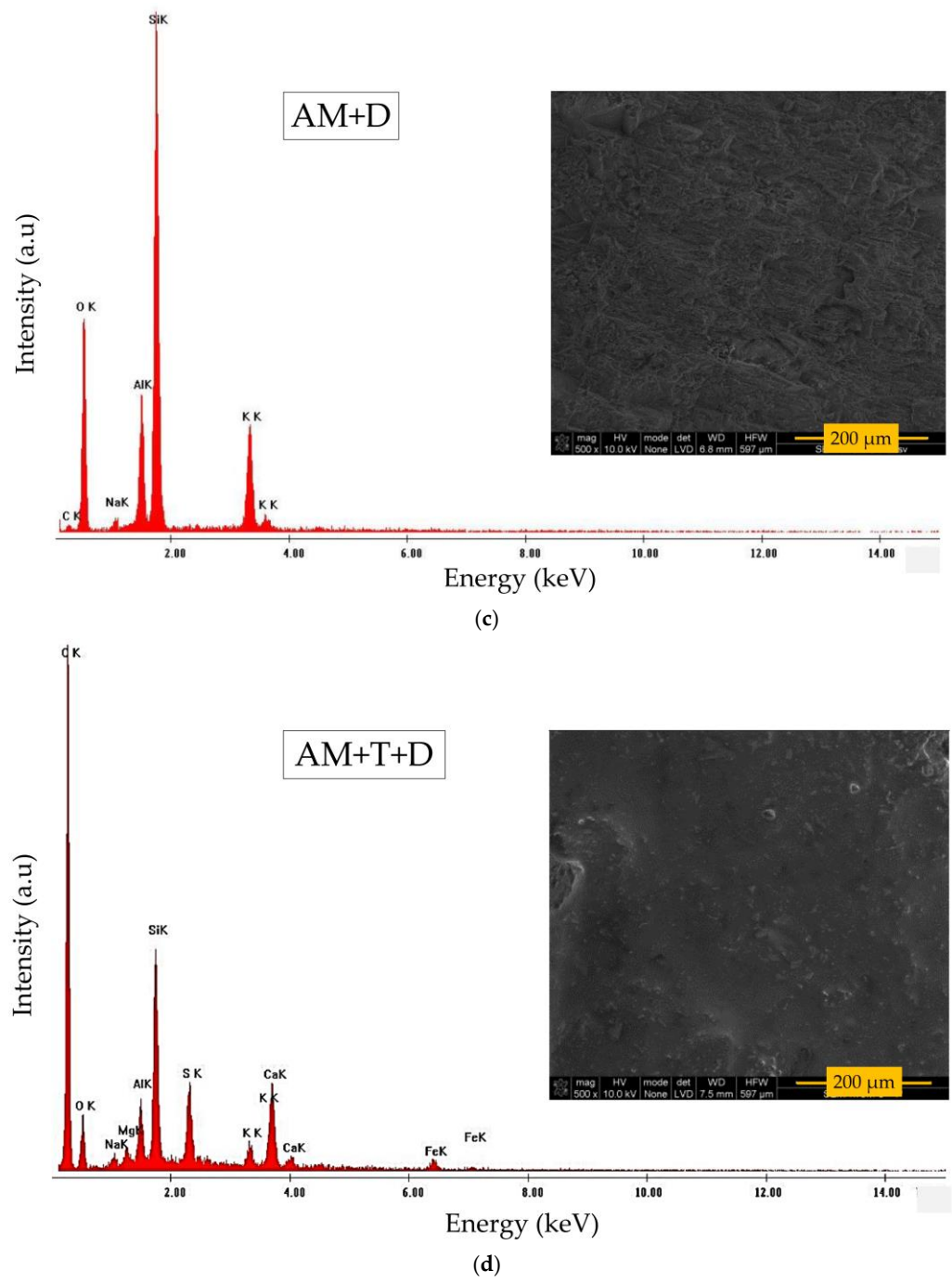
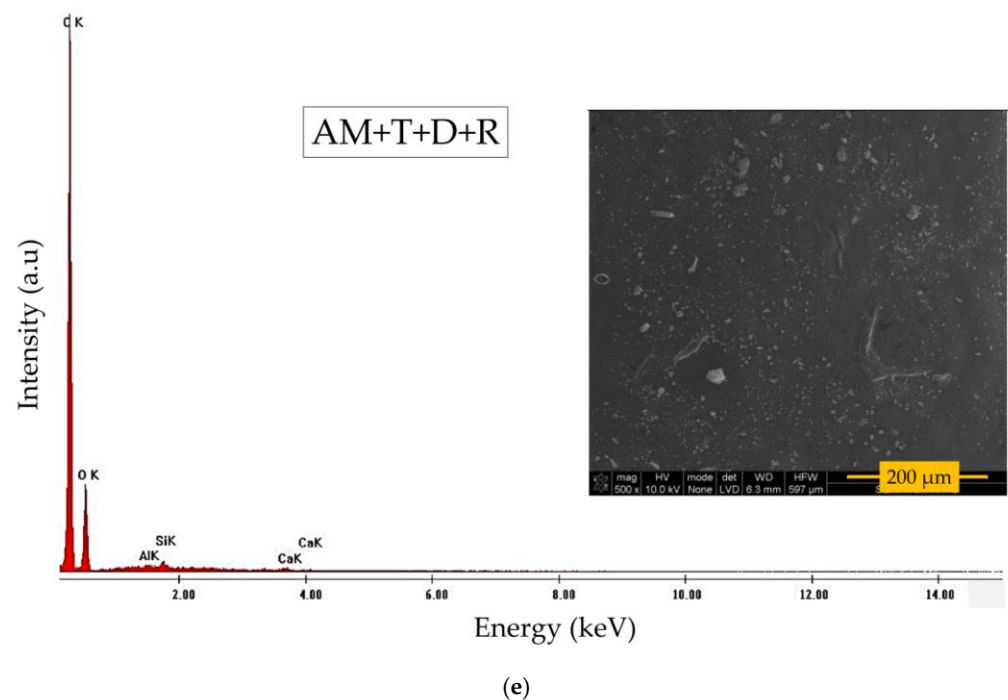


Figure 7. Cont.



**Figure 7.** EDS spectrum and SEM micrograph representation (insert) for the samples: (a) AM, (b) AM+T, and (c) AM+D, (d) AM+T+D, and (e) AM+T+D+R.

In AM+T+D and AM+T+D+R, the micrographic and spectral changes are even more pronounced compared to AM. The asphalt mixture elements become less evident (lower peaks and smoother surface) in both functionalized samples due to the layer formed by TS, especially in the specimen containing resin. The AM+T+D combination results in a decrease of the Si peak in the spectrum and an increase in C amounts (from the TM). In the spectral analysis of AM+T+D+R, the elements belonging to the constitution of the asphalt mixture aggregates have practically no intensity, indicating that the insertion of the resin in the TS causes a greater morphological and chemical change in the specimen surface. The carbon peak in specimen AM+T+D+R is also pronounced due to the presence of thermocapsules.

Thus, the SEM and EDS tests show the changes that functionalization leads to on the surface of the asphalt mixtures, especially in AM+T+D+R. Also, the particles are visually better immobilized in the samples where there is resin within the TS. This is the reason it was added to the TS to be sprayed to improve the immobilization process of the thermocapsules over the substrate.

### 3.4. Quick Ultraviolet Accelerated Weathering Test and Colorimetry on Asphalt Mixture

The color coordinates values,  $L^*$ ,  $a^*$ , and  $b^*$  were collected for dwell times of 0 and 48 h in the Quick Ultraviolet Accelerated Weathering Test (QUV test). The variations  $\Delta E^*$  (see Equation (1)), as well as the  $\Delta L^*$ ,  $\Delta a^*$ , and  $\Delta b^*$  were calculated for the mentioned dwell times in the QUV test, as shown in the results in Table 1.

**Table 1.** Results of the Colorimetry test.

Coordinates	AM+T	AM+D	AM+T+D	AM+D+R	AM+T+R	AM+T+D+R
$\Delta L^*$	0.58	−2.33	1.54	−10.93	−3.29	4.69
$\Delta a^*$	−2.12	0.25	−0.51	0.11	−2.09	1.62
$\Delta b^*$	0.50	−1.55	0.17	−3.24	3.09	4.50
$\Delta E^*$	1.20	2.36	1.54	10.93	7.26	8.66

As expected, the sample AM+T showed the lowest  $\Delta E^*$  values, since both thermocapsules and asphalt mixtures present a dark color at room temperature. Therefore, if there is a degradation of the thermocapsules, the phenomenon cannot be measured using this analysis, since the  $\Delta L^*$  value is relatively low (close to 0), due to the equally dark color of the thermocapsules and the asphalt mixture.

The  $\Delta L^*$  parameter is relevant for observations in the Colorimetry test, since it represents the color variation from black to white. High positive variations in the  $\Delta L^*$  parameter are desirable for the purpose of this functionalization, which is to modify the color of the asphalt mixture surface to lighter colors and thus to reduce its heat absorption and, consequently, the UHI effects.

For sample AM+T+D there is a small increase in the  $\Delta L^*$  parameter, which is due to the degradation of the thermocapsules and thus the exposure of the dye. As for the AM+T+D+R sample, a considerable increase in the  $\Delta L^*$  parameter is observed, as is one of the highest perceptibility factors,  $\Delta E^*$ . This sample is distinguished from the previous one by the inclusion of resin. The addition of resin contributed to a higher degradation of the thermocapsules and, consequently, a higher exposure of the dye.

However, the sample AM+D showed a significant decrease in the  $\Delta L^*$  parameter, indicating that the QUV test also promotes dye degradation. The samples AM+D+R and AM+T+R showed a greater decrease in the  $\Delta L^*$  parameter, which may mean that the QUV test can trigger photochemical reactions between the resin and the other components and thus contribute to their degradation.

### 3.5. Accelerated Polishing Test on Asphalt Mixture

The asphalt mixtures functionalized with TS containing thermocapsules, dye, and resin, after the immersion time, were submitted to three cycles of one hour each in the accelerated polishing equipment. Figure 8 shows the images taken at the beginning of the test and at the end of each cycle.

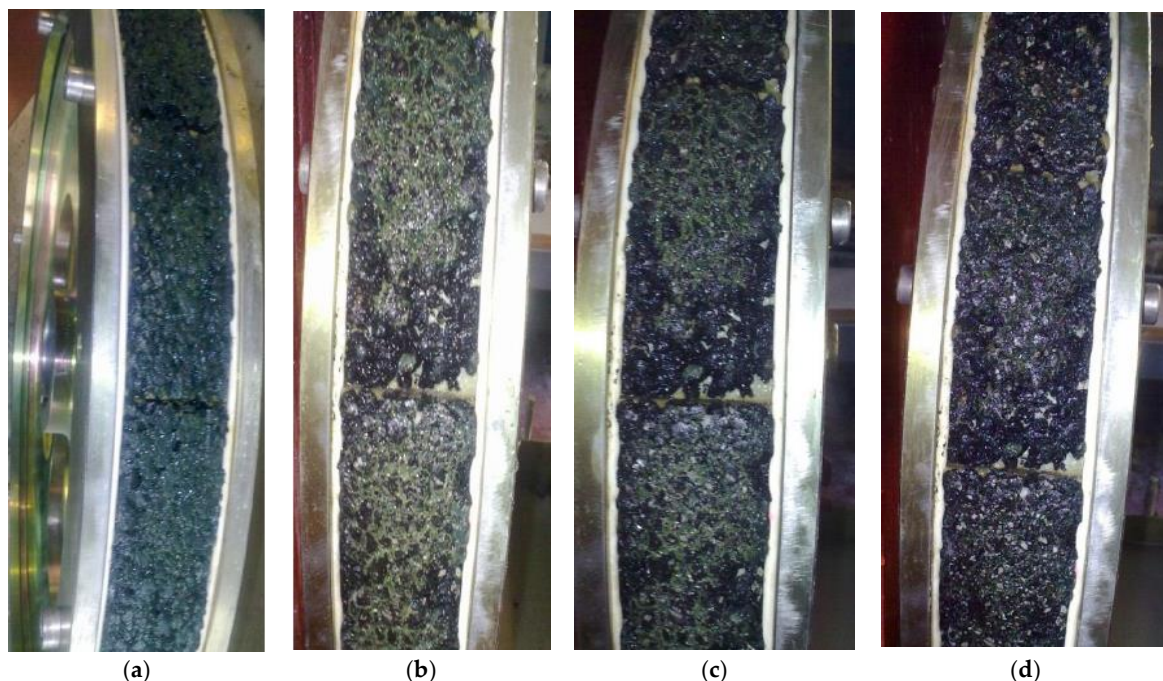


**Figure 8.** Aspect of the specimens functionalized with TS submitted to the Accelerated Polishing Test after  $t$  (hours): (a)  $t = 0$ , (b)  $t = 1$ , (c)  $t = 2$ , and (d)  $t = 3$ .

At the end of the cycles, traces of the surface solution are observed, as can be seen in Figures 8 and 9. It is possible to verify macroscopically that the color emerging from the sample surface is yellowish, coming from the dye in the asphalt mixture. Thus, it



can be assessed that its wear resistance has been ensured. Also, at the end of the test, the asphalt mixtures were partially disintegrated, resulting from the high severity of the wearing conditions, degrading not only the surface coating but also the substrate.

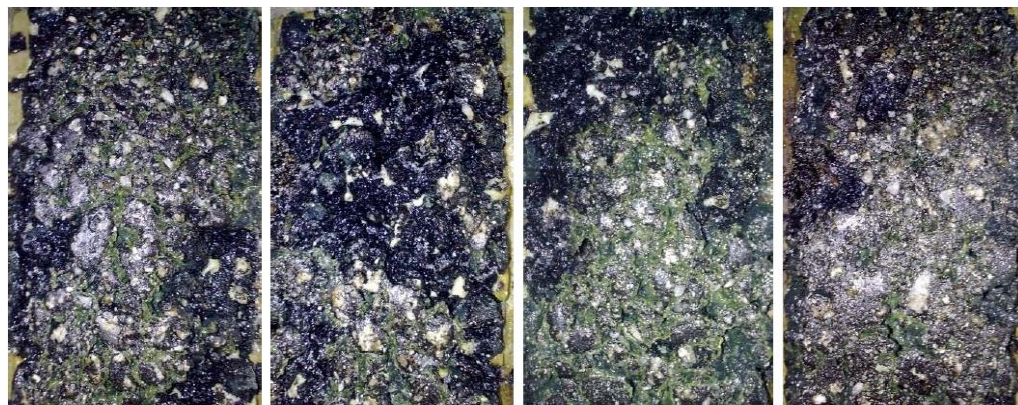


**Figure 9.** Details of the specimens after the Accelerated Polishing Test ( $t = 3$  h).

#### 4. Conclusions

This article was devoted to developing a functionalization coating with TM capable of helping to reduce the UHI effects aggravated by the dark coloration of asphalt pavement. Asphalt substrates (asphalt binder and asphalt mixture) were superficially modified by spraying thermochromic solutions composed of a combination of thermocapsules, dye, and resin. Subsequently, they were subjected to various tests, and the following conclusions were reached:

- From the Fourier Transform Infrared Spectroscopy (FTIR), the characteristic peaks characterize the surface functionalization and, consequently, the presence of the TS over the asphalt substrate.
- The Thermal Differential test confirmed that the activation temperature of the TS occurs at about 30 °C and the reversibility of the thermochromic effect of the TS was ensured.
- The Scanning Electron Microscopy (SEM) micrographs showed that the functionalization caused morphological changes in the surface of the samples, and Energy-Dispersive X-ray Spectrometer (EDS) spectra show the variation of the chemical elements placed on the specimen surface. Such results point to the occurrence of the functionalization, as well as the permanence of the TS on the asphalt surface.
- From the Quick Ultraviolet Accelerated Weathering Test (QUV test), the samples containing solutions sprayed with thermocapsules, dye, and resin showed high values of  $\Delta E^*$  and the largest increases in  $\Delta L^*$ , indicating higher luminosity values, which are potential results to mitigate UHI. The performance of the sample containing only dye on the asphalt mixture surface suggests that the QUV test also promotes some degradation of the dye.
- In the Accelerated Polishing test, the asphalt mixture functionalized with TS presented dye traces on the surface. It is indicative that the functionalization resisted the wear condition even though this is a test that promotes severe wearing and removal of part of the asphalt binder and aggregates.

In summary, the functionalized asphalt substrates showed surface morphological and chemical evidence of TS presence; thermochromic capacity and color reversibility; a noticeable change in the color perceptibility factor and increased luminosity after simulation of environmental degradation; and wear resistance concerning TS immobilization to the substrate was partially conclusive and satisfactory. Thus, it is noticeable that the functionalization has the potential to contribute to reducing energy absorption in asphalt pavement, being a new and feasible capability for mitigating UHI effects, once it is expected that a higher percentage of the light will be reflected more (mainly in the infrared range),

having as a main consequence the mitigation of the sharp rise in pavement temperature. Thus, if used in strategic regions, since more than half the area of urban centers is road pavement and parking lots (and usually asphalt), the effects of the UHI can be mitigated.

However, it is plausible to devote future efforts to studying the effect of this functionalization on pavement friction values, since this impacts the safety of vehicle driving. Furthermore, new methods for immobilization of the TS need to be studied and an analysis carried out of the maintenance of the thermochromic capacity of the functionalized asphalt mixture after mechanical wear. Finally, a study of the behavior of the surface temperatures of the functionalized pavement is needed to verify the real gains in terms of decreasing energy absorption compared to non-functionalized pavements.

**Author Contributions:** Conceptualization, J.C. and E.F.; methodology, J.C., E.F. and P.C.; validation, J.C., E.F., I.R.S., S.L.J. and J.H.O.N.; formal analysis, P.C., O.L.J., J.C., E.F. and I.R.S.; investigation, P.C., E.F. and J.C.; resources, E.F. and J.C.; data curation, P.C.; writing—original draft preparation, O.L.J.; writing—review and editing, E.F., L.M., J.C., I.R.S., O.L.J., É.M., J.H.O.N. and S.L.J.; visualization, P.C., I.R.S. and O.L.J.; supervision, E.F. and J.C.; project administration, J.C. and E.F.; funding acquisition, E.F. and J.C.; All authors have read and agreed to the published version of the manuscript.

**Funding:** This research was funded namely by the Portuguese Foundation for Science and Technology (FCT), NanoAir PTDC/FISMAC/6606/2020, MicroCoolPav EXPL/EQU-EQU/1110/2021, UIDB/04650/2020, and UIDB/04029/2020. This research was also supported by the doctoral Grant PRT/BD/154269/2022 financed by the Portuguese Foundation for Science and Technology (FCT), and with funds from POR Norte-Portugal 2020 and State Budget, under MIT Portugal Program. The fourth author would like to acknowledge the FCT for funding (2022.00763.CEECIND).

**Institutional Review Board Statement:** Not applicable.

**Informed Consent Statement:** Not applicable.

**Data Availability Statement:** Not applicable.

**Conflicts of Interest:** The authors declare no conflict of interest.

## References

1. Segundo, I.R.; Freitas, E.; Branco, V.T.F.C.; Landi, S.; Costa, M.F.; Carneiro, J.O. Review and analysis of advances in functionalized, smart, and multifunctional asphalt mixtures. *Renew. Sustain. Energy Rev.* **2021**, *151*, 111552. [[CrossRef](#)]
2. Geng, X.; Zhang, D.; Li, C.; Yuan, Y.; Yu, Z.; Wang, X. Impacts of climatic zones on urban heat island: Spatiotemporal variations, trends, and drivers in China from 2001–2020. *Sustain. Cities Soc.* **2022**, *89*, 104303. [[CrossRef](#)]
3. Zhao, L.; Lee, X.; Smith, R.B.; Oleson, K. Strong contributions of local background climate to urban heat islands. *Nature* **2014**, *511*, 216–219. [[CrossRef](#)] [[PubMed](#)]
4. Santero, N.J.; Horvath, A. Global warming potential of pavements. *Environ. Res. Lett.* **2009**, *4*, 34011. [[CrossRef](#)]
5. Stephens, G.L.; O'Brien, D.; Webster, P.J.; Pilewski, P.; Kato, S.; Li, J. The albedo of Earth. *Rev. Geophys.* **2015**, *53*, 141–163. [[CrossRef](#)]
6. Coakley, J.A. Reflectance and albedo, surface. In *Encyclopedia of Atmospheric Sciences*, 1st ed.; Elsevier: Amsterdam, The Netherlands, 2003; pp. 1914–1923.
7. Mohajerani, A.; Bakaric, J.; Jeffrey-Bailey, T. The urban heat island effect, its causes, and mitigation, with reference to the thermal properties of asphalt concrete. *J. Environ. Manag.* **2017**, *197*, 522–538. [[CrossRef](#)] [[PubMed](#)]
8. Santamouris, M. Using cool pavements as a mitigation strategy to fight urban heat island—A review of the actual developments. *Renew. Sustain. Energy Rev.* **2013**, *26*, 224–240. [[CrossRef](#)]
9. Wang, Z.; Xie, Y.; Mu, M.; Feng, L.; Xie, N.; Cui, N. Materials to Mitigate the Urban Heat Island Effect for Cool Pavement: A Brief Review. *Buildings* **2022**, *12*, 1221. [[CrossRef](#)]
10. Yan, X.; Wang, L.; Qian, X. Effect of Coating Process on Performance of Reversible Thermochromic Waterborne Coatings for Chinese Fir. *Coatings* **2020**, *10*, 223. [[CrossRef](#)]
11. Garshasbi, S.; Santamouris, M. Using advanced thermochromic technologies in the built environment: Recent development and potential to decrease the energy consumption and fight urban overheating. *Sol. Energy Mater. Sol. Cells* **2019**, *191*, 21–32. [[CrossRef](#)]
12. Seeboth, A.; Löttsch, D.; Ruhmann, R. First example of a non-toxic thermochromic polymer material—Based on a novel mechanism. *J. Mater. Chem. C* **2013**, *1*, 2811. [[CrossRef](#)]
13. Pulit-Prociak, J.; Banach, M. Silver nanoparticles—A material of the future . . . ? *Open Chem.* **2016**, *14*, 76–91. [[CrossRef](#)]



14. Yan, X.; Chang, Y.; Qian, X. Effect of the Concentration of Pigment Slurry on the Film Performances of Waterborne Wood Coatings. *Coatings* **2019**, *9*, 635. [[CrossRef](#)]
15. Tözüm, M.S.; Aksoy, S.A.; Alkan, C. Microencapsulation of Three-Component Thermochromic System for Reversible Color Change and Thermal Energy Storage. *Fibers Polym.* **2018**, *19*, 660–669. [[CrossRef](#)]
16. Berardi, U.; Garai, M.; Morselli, T. Preparation and assessment of the potential energy savings of thermochromic and cool coatings considering inter-building effects. *Sol. Energy* **2020**, *209*, 493–504. [[CrossRef](#)]
17. Cheng, Y.; Zhang, X.; Fang, C.; Chen, J.; Wang, Z. Discoloration mechanism, structures and recent applications of thermochromic materials via different methods: A review. *J. Mater. Sci. Technol.* **2018**, *34*, 2225–2234. [[CrossRef](#)]
18. Morini, E.; Castellani, B.; Nicolini, A.; Rossi, F.; Berardi, U. Effects of aging on retro-reflective materials for building applications. *Energy Build.* **2018**, *179*, 121–132. [[CrossRef](#)]
19. Karlessi, T.; Santamouris, M.; Apostolakis, K.; Synnefa, A.; Livada, I. Development and testing of thermochromic coatings for buildings and urban structures. *Sol. Energy* **2009**, *83*, 538–551. [[CrossRef](#)]
20. Yan, X.; Wang, L.; Qian, X. Influence of Thermochromic Pigment Powder on Properties of Waterborne Primer Film for Chinese Fir. *Coatings* **2019**, *9*, 742. [[CrossRef](#)]
21. Pan, P.; Yan, X.; Zhao, W. Effect of Coating Process of Photochromic and Thermochromic Composite Microcapsules on Coating Properties for Basswood. *Coatings* **2022**, *12*, 1246. [[CrossRef](#)]
22. Anupam, B.R.; Sahoo, U.C.; Chandrappa, A.K.; Rath, P. Emerging technologies in cool pavements: A review. *Constr. Build. Mater.* **2021**, *299*, 123892. [[CrossRef](#)]
23. Li, F.; Zhou, S.; Du, Y.; Zhu, X.; Yu, J.; Fu, K.; Yang, Z. Experimental study on heat-reflective epoxy coatings containing nano-TiO<sub>2</sub> for asphalt pavement resistance to high-temperature diseases and CO/HC emissions. *J. Test. Eval.* **2019**, *47*, 2765–2775. [[CrossRef](#)]
24. Chen, Y.; Li, Z.; Ding, S.; Yang, X.; Guo, T. Research on heat reflective coating technology of asphalt pavement. *Int. J. Pavement Eng.* **2022**, *23*, 4455–4464. [[CrossRef](#)]
25. Zhang, X.; Li, H.; Xie, N.; Jia, M.; Yang, B.; Li, S. Laboratorial Investigation on Optical and Thermal Properties of Thermochromic Pavement Coatings for Dynamic Thermoregulation and Urban Heat Island Mitigation. *Sustain. Cities Soc.* **2022**, *83*, 103950. [[CrossRef](#)]
26. Hu, J.; Gao, Q.; Yu, X. Characterization of the optical and mechanical properties of innovative multifunctional thermochromic asphalt binders. *J. Mater. Civ. Eng.* **2015**, *27*, 4014171. [[CrossRef](#)]
27. Hu, J.; Yu, X. Innovative thermochromic asphalt coating: Characterisation and thermal performance. *Road Mater. Pavement Des.* **2016**, *17*, 187–202. [[CrossRef](#)]
28. Yu, B.; Peng, W.; Liu, J.; Zhang, J.; Li, W.; Hong, Q. Research on the performance of temperature responsive asphalt mixture with thermochromic material. *Road Mater. Pavement Des.* **2022**, *23*, 713–724. [[CrossRef](#)]
29. Chen, Z.; Zhang, H.; Duan, H.; Shi, C. Improvement of thermal and optical responses of short-term aged thermochromic asphalt binder by warm-mix asphalt technology. *J. Clean. Prod.* **2021**, *279*, 123675. [[CrossRef](#)]
30. Decky, M.; Papanova, Z.; Juhas, M.; Kudelcikova, M. Evaluation of the Effect of Average Annual Temperatures in Slovakia between 1971 and 2020 on Stresses in Rigid Pavements. *Land* **2022**, *11*, 764. [[CrossRef](#)]
31. Yi, Y.; Jiang, Y.; Tian, T.; Fan, J.; Bai, C.; Deng, C.; Xue, J.; Ji, X. Attenuation pattern of skid resistance of heat reflective coatings under the effect of simulated pavement abrasion. *Int. J. Pavement Eng.* **2022**, *23*, 1–12. [[CrossRef](#)]
32. Homem, N.C.; Yamaguchi, N.U.; Vieira, M.F.; Amorim, M.T.S.P.; Bergamasco, R. Surface modification of microfiltration membrane with GO nanosheets for dyes removal from aqueous solutions. *Chem. Eng. Trans.* **2017**, *60*, 259–264. [[CrossRef](#)]
33. Yan, X.; Chang, Y. Investigation of waterborne thermochromic topcoat film with color-changing microcapsules on Chinese fir surface. *Prog. Org. Coat.* **2019**, *136*, 105262. [[CrossRef](#)]
34. Yan, X.; Wang, L.; Qian, X. Influence of the PVC of Glass Fiber Powder on the Properties of a Thermochromic Waterborne Coating for Chinese Fir Boards. *Coatings* **2020**, *10*, 588. [[CrossRef](#)]
35. Zhang, H.; Chen, Z.; Li, L.; Zhu, C. Evaluation of aging behaviors of asphalt with different thermochromic powders. *Constr. Build. Mater.* **2017**, *155*, 1198–1205. [[CrossRef](#)]
36. Garcia, A.; Jelfs, J.; Austin, C.J. Internal asphalt mixture rejuvenation using capsules. *Constr. Build. Mater.* **2015**, *101*, 309–316. [[CrossRef](#)]
37. Robertson, A.R. The CIE 1976 color-difference formulae. *Color Res. Appl.* **1977**, *2*, 7–11. [[CrossRef](#)]
38. Malm, V.; Strååt, M.; Walkenström, P. Effects of surface structure and substrate color on color differences in textile coatings containing effect pigments. *Text. Res. J.* **2013**, *84*, 125–139. [[CrossRef](#)]
39. ASTM D3319-11; Standard Practice for the Accelerated Polishing of Aggregates Using the British Wheel. ASTM: West Conshohocken, PA, USA, 1997.
40. Woolley, J.T. Reflectance and transmittance of light by leaves. *Plant Physiol.* **1971**, *47*, 656–662. [[CrossRef](#)]
41. Rocha Segundo, I.; Landi, S., Jr.; Margaritis, A.; Pipintakos, G.; Freitas, E.; Vuye, C.; Blom, J.; Tytgat, T.; Denys, S.; Carneiro, J. Physicochemical and rheological properties of a transparent asphalt binder modified with nano-TiO<sub>2</sub>. *Nanomaterials* **2020**, *10*, 2152. [[CrossRef](#)]
42. Xu, T.; Huang, X. Study on combustion mechanism of asphalt binder by using TG-FTIR technique. *Fuel* **2010**, *89*, 2185–2190. [[CrossRef](#)]

43. Doblies, A.; Boll, B.; Fiedler, B. Prediction of Thermal Exposure and Mechanical Behavior of Epoxy Resin Using Artificial Neural Networks and Fourier Transform Infrared Spectroscopy. *Polymers* **2019**, *11*, 363. [[CrossRef](#)] [[PubMed](#)]
44. Xu, S.; Zou, L.; Ling, X.; Wei, Y.; Zhang, S. Preparation and thermal reliability of methyl palmitate/methyl stearate mixture as a novel composite phase change material. *Energy Build.* **2014**, *68*, 372–375. [[CrossRef](#)]
45. González, M.G.; Cabanelas, J.C.; Baselga, J. Applications of FTIR on epoxy resins-identification, monitoring the curing process, phase separation and water uptake. *Infrared Spectrosc. Sci. Eng. Technol.* **2012**, *2*, 261–284.
46. Wei, J.B.; Shull, J.C.; Lee, Y.-J.; Hawley, M.C. Characterization of Asphalt Binders Based on Chemical and Physical Properties. *Int. J. Polym. Anal. Charact.* **1996**, *3*, 33–58. [[CrossRef](#)]
47. Cherdoud-Chihani, A.; Mouzali, M.; Abadie, M.J.M. Study of crosslinking AMS/DGEBA system by FTIR. *J. Appl. Polym. Sci.* **1998**, *69*, 1167–1178. [[CrossRef](#)]
48. Shukla, R.; Kumar, P. Self-curable epoxide resins based on cardanol for use in surface coatings. *Pigment Resin Technol.* **2011**, *40*, 311–333. [[CrossRef](#)]

**Disclaimer/Publisher’s Note:** The statements, opinions and data contained in all publications are solely those of the individual author(s) and contributor(s) and not of MDPI and/or the editor(s). MDPI and/or the editor(s) disclaim responsibility for any injury to people or property resulting from any ideas, methods, instructions or products referred to in the content.